# Supporting Information


## Boitard et al. 10.1073/pnas.1200894109


### SI Material and Methods

**Strains and Culture Conditions.** Strains used in this study are described in Table S2. Glucose concentration varied from 20 to 200 g/L. For single-cell experiments based on leucine auxotrophy, cells were grown in nonrestrictive medium (synthetic defined, SD all) until they reached exponential phase. They were then washed in restrictive medium (SD-L) three times and incubated for 2 h at 30 °C in SD-L. They were then encapsulated inside droplets and stored at 30 °C.

For single-cell experiments based on the thermosensitive mutant *cdc28*, cells were grown in SD-all at permissive temperature (30 °C) until they reached exponential phase. They were then encapsulated and maintained at restrictive temperature (38 °C).

**Formulation.** The continuous phase is a mixture of 52% (wt/wt) of mineral oil (Sigma) and 48% (wt/wt) of highly purified perfluorohexyloctane (F6H8; Fluoron GmbH). To stabilize the emulsion, we added 0.5% (wt/wt) span80 (Sigma Aldrich) and 0.25% (wt/wt) of ArlacelP125 (Croda).

F6H8 acts as a bad solvent for the surfactants which promotes adhesion between the droplets, creating a surfactant bilayer at the contact interface (Fig. S1).

Above 50% (wt/wt) of F6H8, ArlacelP125 is not soluble in the oil mixture anymore. The main advantage compared to a nonadhesive emulsion is that the distance between drops is totally controlled by the adhesion, which only depends on the formulation. In the case of nonadhesive droplets the distance (thickness of the oil film) depends on the compaction of the emulsion, which is poorly reproducible from one experiment to the next. Hence, the use of adhesive emulsion provides robustness to the procedure.

**Device Manufacturing and Operation.** For the droplet generation, we used a flow-focusing design (Fig. S3*A*). Flows were controlled with syringe pumps (Harvard Apparatus). The typical flow rates for the aqueous phase was 80–100 μL/ min and for the continuous phase 400 μL/h. To compact the droplets inside the incubation chamber, we extracted some of the continuous phase with syringe pump in withdraw mode at −350 μL/h. We obtained a compact two-dimensional network as illustrated in Fig. S3*C*.

The 25-μm-deep incubation chamber (Fig. S2*B*) was custom-made by gluing microscope glass slides together, separated by 25-μm-thin wires (Omega). Ports of the chamber were drilled in the top slide and glued with Nanoport (Upchurch Scientific) to provide for a connection from the microfluidic chip to the chamber. To avoid wetting of the drops on the walls of the chamber, this latter was silanized with a perfluorosilane (Sigma). Once the chamber was filled with the droplets, the chip was disconnected and the chamber plugged.

**Image Analysis.** Images were processed with custom software written in Matlab. After a thresholding step, only the contour of the droplets were kept from the binary images (Fig. S7 *A.a* and *A.b*). Volume of the pancake-shaped droplets was then calculated according to the following equation: $V = 2\pi r(R-r)^2 + \pi^2 r^2\left[R - r\left(1-\frac{3}{4\pi}\right)\right]$ where $r = \frac{h}{2}$ depends on the height of the chamber. The different parameters are illustrated in Fig. S7*A.c*. As illustrated in Fig. S7*B*, for isolated empty drops, we observed a change in volume during the first 200 min of the experiment. This effect was seen on every drop of the network, and we suppose it resulted from the relaxation of the system. To correct for this volume variation unrelated to biological processes, we selected an empty isolated drop as a reference droplet and used its volume to normalize the other droplets. Hence, $V_{\text{corrected}} = V(t)V^0_{\text{ref}}/V_{\text{ref}}$. This correction is particularly important for single-cell experiments where volume variation is very small.

**Cell Size Measurement.** To estimate cell size inside the droplets, we measured segmented cell boundaries as described in Fig. S6 where size $= (\text{area})^{3/2}$. The error on the measured area was 15 pixels, resulting in an error of 58 pixel$^{3/2}$ for the size.

Cell size distributions were deduced (Fig. S6) with the following coefficient of variation: $\text{CV}(2N) = 30\%$; $\text{CV}(3N) = 20\%$; $\text{CV}(4N) = 23\%$.

**Osmolarity Measurements.** Because the flux between drops was set by osmolarity gradients, we measured the initial osmolarity of the media with a cryogenic osmometer (Gonotec; Osmomat 030). For example, an SD medium containing $C_g = 100$ g/mol $= 555$ mosmol/L had an osmolarity $C_0 = C_g + C_{ng} =$ 712 mosmol/L. The "1X" corresponds to the normal concentration of nonglucose nutrients. The "2X" stands for twice the normal concentration. The concentration of glucose in each medium is given in g/L. The L stands for "without leucine."


1. Schmitz CHJ, Rowat AC, Köster S, Weitz DA (2009) Dropspots: A picoliter array in a microfluidic device. *Lab Chip* 9:44–49.


| Medium (SD) | 1X-20 g/L | 1X-20 g/L-L | 1X-50 g/L | 1X-100 g/L | 2X-100 g/L | 1X-150 g/L | 1X-200 g/L |
|---|---|---|---|---|---|---|---|
| Osmolarity (mosmol.L$^{-1}$) | 254 | 250 | 429 | 772 | 849 | 1,090 | 1,502 |

### Diffusion Model and Parameters

**Without Cells.** A semipermeable membrane separates two reservoirs containing, respectively, $c_1$ and $c_2$ g/L of glucose. According to Fick's law, the flow of a water molecule across the membrane is given by $j = -D_m \nabla c_m$ where $D_m$ is the diffusion coefficient of water in the membrane and $\nabla c_m$ is the concentration gradient across the membrane. According to Overton's rule, $\nabla c_m = K_p \frac{c_2 - c_1}{d}$ where $K_p$ is the partition coefficient of the nondiffusible molecule (glucose, for instance) inside the membrane and $d$ the membrane thickness. We can write $j = P(c_2 - c_1) = P\nabla c$ where $P = \frac{D_m K_p}{d}$ is the permeability. The amount of water molecules that cross the surface $A$ during time $dt$ is $jAdt = \frac{dv}{v_w}$, where $dv$ is the volume change and $v_m$ is the molar volume of water. The water flow across the surface of diffusion $A$ is then written as $\frac{dv}{dt} = -PAv_w\Delta c$. As illustrated in Fig. S1, the area $A$ of the adhesive patch between the droplets is mainly fixed by the formulation of the emulsion. So, we finally write $\frac{dv}{dt} = -Fv_w\Delta c$ where $F$ is the flow parameter that is proportional

to the number of contacts. To measure this transport parameter $F$, we achieved a model experiment where we put in contact two droplets containing 20 and 5 g/L of glucose, respectively. We measured the volume variation of the less concentrated drop (Fig. 1*A*). The final volume confirms that the interface between the drop is not permeable to glucose but only to water. By fitting those results with the transport equation we estimated the flow parameter to be $F \sim 40$ pL·min$^{-1}$ per contact in the adhesive formulation. We did the same measurement for a nonadhesive formulation as described by Schmitz et al. (1) and found in the case of a closed-packed emulsion (ideal case where the distance between the droplets is the smallest and the surface of contact maximized) $F \sim 13$ pL·min$^{-1}$ per contact.

Finally, we verified that ethanol diffuses faster than water (Fig. S2 and Movie S2). If water diffuses faster than ethanol, then drop B should empty itself in drop A, which we did not observe.

**With Cells.** We modeled droplet contraction of yeast containing droplets by incorporating the expression of substrate consumption in the transport model.

In the glucose-limited regime, the amount of substrate can be written $s(t) = s_0 - \frac{\beta(t)}{Y_{ng}} - \frac{\beta(t)}{Y_g}$ where $Y_{ng}$ and $Y_g$ are, respectively, the biomass yields for nonglucose and glucose; $\beta(t)$ is the biomass at time $t$.

In experiments where glucose is not the limiting nutrient, the yeast divides until it has consumed all the limiting nutrient (time $t_c$) and produced a certain amount of biomass $\beta_c$. Before $t_c$, $s(t)$ has the same expression as in the glucose-limited regime. If we call $q_m$ the maintenance energy, that is, the glucose consumed by nondividing cells after $t_c$, then

$$s(t) = s_0 - \frac{\beta_c}{Y_{ng}} - \frac{\beta_c}{Y_g} - \beta_c q_m t. \qquad \textbf{[S1]}$$

We verified that this model provided a satisfying description of the data (Fig. S8*A*). We then used it to identify the sources of the dispersion among experimental curves, by varying the initial volume, the initial number of cells inside the drops, or the number of contacts in the model (Fig. S8*B*).

## Nutrient Consumption Calculation

For different initial glucose concentrations, we measured the final contraction of every nursing droplet (see Table S1) and initial concentrations (see *Cell Size Measurement*). Knowing the volume, we deduce the final amount of nutrients $s_{ss}$ and the initial amount of nutrients $s_0$.

The amount of nutrients that were consumed is calculated as $s_0 - s_{ss} = s_0\left(1 - \frac{V_{ss}}{V_0}\right)$ and is plotted as a function of the initial glucose concentration. Fig. S4 suggests that all the glucose is consumed.

## Maintenance Energy Evaluation

The maintenance energy was measured from experiments where cells had stopped dividing but continued to consume glucose. In this regime there is a relationship between droplets volume variation and substrate variation: $\frac{\Delta V}{V_0} = \frac{\Delta s}{s_0}$. Hence the slope $p'$ measured from normalized volume can be linked to the slope $p = \beta_c q_m$ in Eq. **S1**: $p' = \beta_c q_m / s_0$. We measured $p'$ in three different cases (Fig. S5): for experiments (*i*) in 1X SD with 100 g/L of glucose, (*ii*) 1X SD with 200 g/L of glucose, and (*iii*) 2X SD with 100 g/L of glucose. Results are represented in Fig. S5.

In case (*ii*), adding twice the amount of sugar comes to have twice the initial amount of substrate, $2s_0$; and in case (*iii*), adding twice the amount of nonglucose medium comes to doubling the amount of biomass produced, $2\beta_c$. We verified $q(i) = 2\,q(ii) = 1/2\,q(iii)$.

From the 1X SD with 100 g/L glucose measurement, we deduced the maintenance energy. Initial substrate quantity $q_m = p's_0/\beta_c$ is the glucose consumption by biomass unit with $\beta_c = 40 \pm 5$ cellules (estimated by counting in the drop); $s_0 = V_0 c_0 = 80$ pL $\times$ 0.712 osmol/L is the initial substrate quantity; $p's_0$ is the amount of nutrient that has been consumed while the cells are not dividing. We assume that the vast majority is glucose. Initial substrate quantity $s_0$ is then converted in glucose equivalent by multiplying by the glucose molar mass (180 g/mol). We find $q_m = 8.10^{-4} \times 80/40 \times 0{,}712.10^{-12} \times 180 \sim 0.2$ pg (glucose)/cell/ min.

For single-cell experiments, the maintenance energy was calculated similarly as $q_m = p's_0/\beta_c$, $\beta_c$, being equal to 1. Initial substrate quantity $s_0$ is deduced from osmolarity measurements.

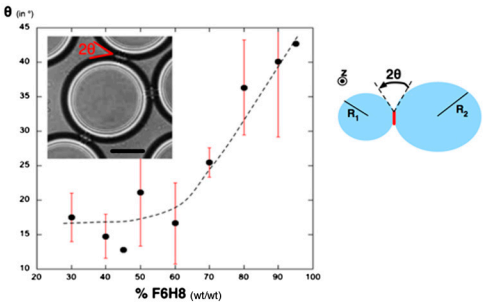


**Fig. S1.** Contact angle (wetting) between two adhesive droplets as a function of additive concentration. The oil mixture contains 0.5% (wt/wt) Span80 in mineral oil. Concentration of F6H8 is changed from 30% to 95%. (Scale bar: 25 μm.)

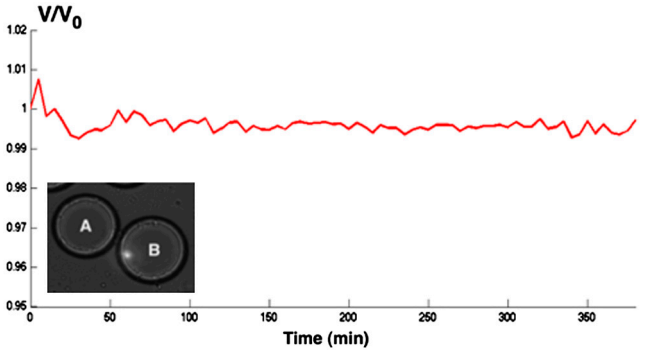


**Fig. S2.** Volume evolution for an ethanol mismatch. Drop B contains 500 mosmol·L$^{-1}$ of sugar and salt and 1 M of ethanol; drop A contains 500 mosmol·L$^{-1}$ of sugar and salt.

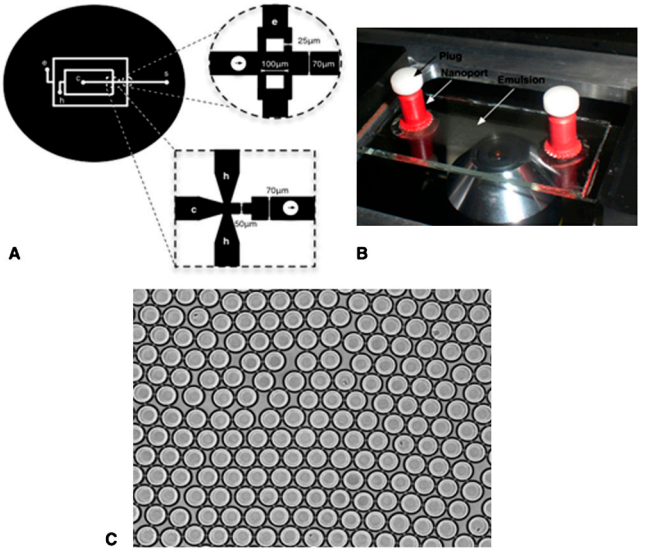


**Fig. S3.** Microfluidic systems for creating a two-dimensional emulsion network. (*A*) Microfluidic chip for droplet generation. Top zoom is the extraction region. Bottom zoom is the flow-focusing region; e, extraction line; h, continuous phase line; c, dispersed phase (+cells) line; s, exit line. (*B*) Glass chamber for monitoring emulsion is 25-μm deep. (*C*) Two-dimensional adhesive emulsion network. The droplets are 50 μm in diameter.

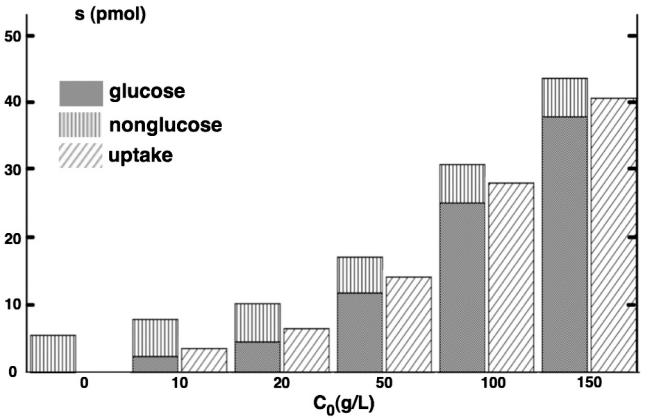


**Fig. S4.** Glucose uptake as a function a initial glucose concentration. Bars on the left correspond to the initial quantities of glucose and nonglucose nutrients (for details see *Nutrient Consumption Calculation*).

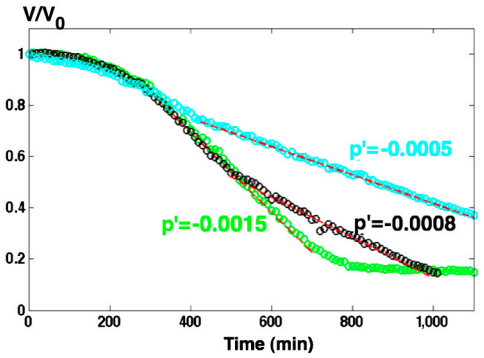


**Fig. S5.** Glucose consumption by a small yeast colony at various substrate concentrations. Each curve represents an average of over 200 experimental curves, CV was 10%. Black, 100 g/L glucose, 1X medium. Green, 100 g/L of glucose, 2X medium. Blue, 200 g/L of glucose, 1X medium.

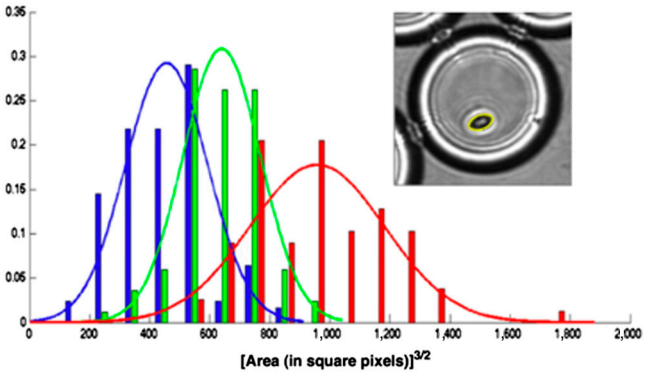


**Fig. S6.** Cell size distribution for diploid (blue), triploid (green), and tetraploid (red) cells. Plain lines, Gaussian fit; mean$(2n) = 456$; mean$(3n) = 640$; mean$(4n) = 957$. (*Inset*) Segmentation of cell boundary.

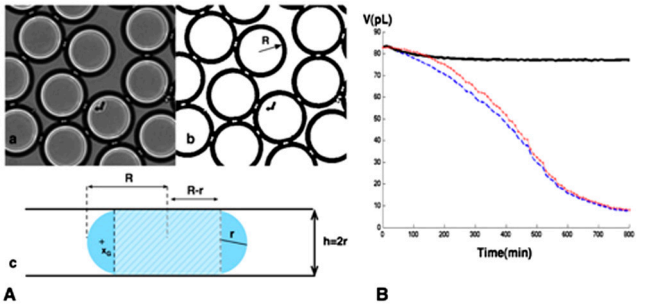


**Fig. S7.** Image analysis, volume calculation, and correction. (*A*) *a*, original image; *b*, binarized image; *c*, geometric sketch of the drop as seen from the side. (*B*) Relaxation of the system illustrated by the volume of an empty drop (black). Nursing drop before correction (blue) and after (see Fig. S1*D*, red).

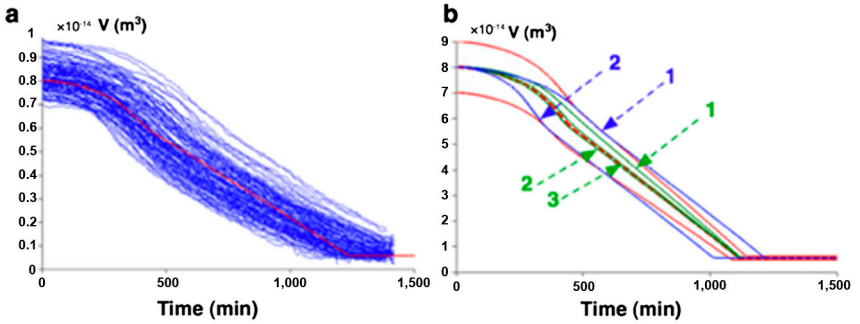


**Fig. S8.** Comparison between model and experimental data. (*A*) Nonglucose limited regime (150 g/L glucose), 146 experimental curves (blue), a model curve (red) for $Y = 0.15$ g(biomasse)/g(glucose); $\tau = 120$ min; $q_m = 0.16$ pg (glucose)·cell$^{-1}$· min$^{-1}$; $F = 4 \times 40$ pL. min$^{-1}$. (*B*) Curves obtained from the model using, for all curves, $Y = 0.15$ g(biomasse)/g(glucose); $\tau = 120$ min; $q_m = 0.16$ pg (glucose)·cell$^{-1}$· min$^{-1}$ and $F = c \times 40$ pL· min$^{-1}$ with $c$ the number of contacting droplets; $c = 1, 2, 3$ (green) or 4 (dashed red) contacts; with $c = 4$ but different initial volumes (red); and with $c = 4$ and one or two initial cells (blue).

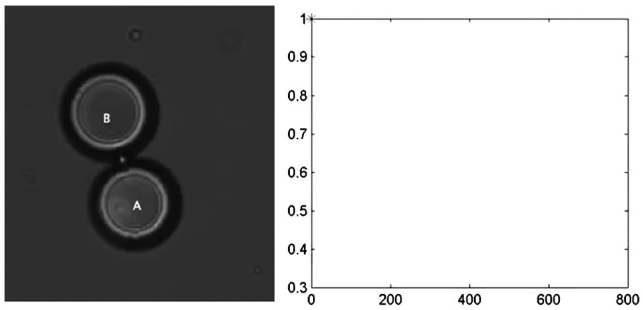


**Movie S1.** Osmotic ripening: model experiment. A 5 g/L glucose-containing droplet (*A*) is emptying itself in a 20 g/L glucose-containing droplet (*B*). The plot on the right side represents the normalized volume evolution of the 5 g/L glucose-containing droplet. Water equilibrates the concentrations diffusing from the less concentrated droplet toward the most concentrated one.

Movie S1 (MOV)

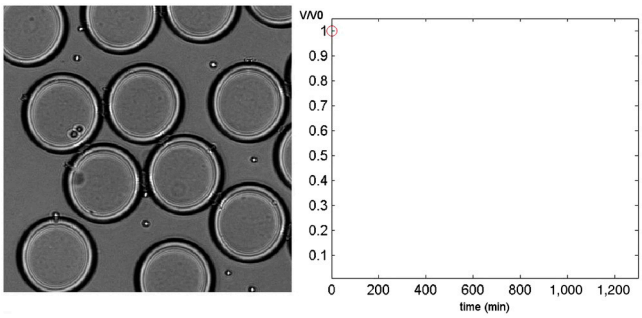


**Movie S2.** Osmotic ripening: yeast experiment. Budding *Saccharomyces cerevisiae* (GY613) cell encapsulated in a 50 g/L glucose-containing synthetic-defined culture medium droplet. As the cell divides, the droplet is emptying itself in the surrounding nonoccupied droplets. The plot on the right side represents the normalized volume evolution of the yeast-containing droplet.

Movie S2 (MOV)

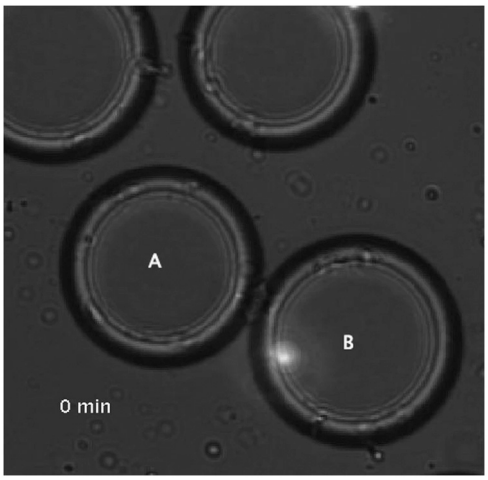


**Movie S3.** Osmotic ripening: model experiment with ethanol. A 50 g/L glucose-containing droplet (*Left*) is brought in contact with a droplet (*Right*) containing the same amount of salt and glucose but with 1 M of ethanol. Ethanol equilibrates faster than water so that no volume change is observed.

Movie S3 (MOV)

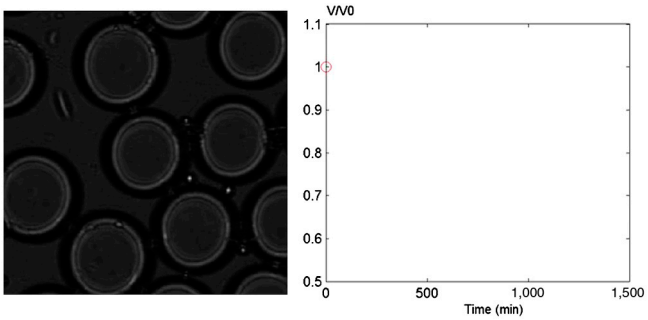


**Movie S4.** Osmotic ripening: bacteria experiment. An *Escherichia coli* cell is encapsulated in M9 medium containing 45 g/L of glucose. After a small increase in volume, the droplet is emptying itself in the surrounding nonoccupied droplets. The plot on the right side represents the normalized volume evolution of the bacteria-containing droplet.

Movie S4 (MOV)

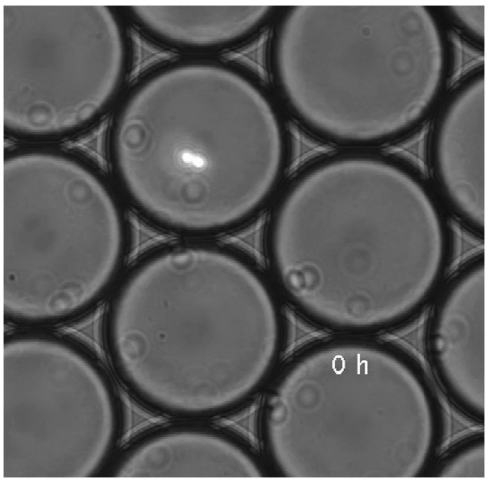


**Movie S5.** Osmotic ripening: enzyme experiment. A droplet containing BSA and protease *K* (highlighted by fluorescent beads) is brought in contact with droplets containing the same amount of BSA. As BSA is digested, the drop inflates.

Movie S5 (MOV)

**Table S1 Osmotic contraction at steady state for various glucose concentrations**

| Medium (SD) | 1X-10 g/L | 1X-20 g/L | 1X-50 g/L | 1X-100 g/L | 1X-150 g/L | 1X-200 g/L |
|---|---|---|---|---|---|---|
| $V_{ss}/V_0$ | 0.55 | 0.35 | 0.18 | 0.09 | 0.065 | 0.045 |

Values are the means over 100 nursing droplets. Coefficient of variation was 10%.

**Table S2. Strains used in this study**

| Name | Ploidy | General background | Genotype | Source |
|---|---|---|---|---|
| GY613 | 2N | RM11-1a | ***MATa/MATalpha****leu2Δ0/leu2Δ0 ura3Δ0/ura3Δ0 hoΔ::KanMX/hoΔ::KanMX amn1-A1103T/amn1-A1103T HIS3::(natMX + Ppgk-yEGFP3)::HIS3/HIS3* | this work |
| GY814 | 2N | S288c | ***MATa/MATa*** *his3Δ1/his3Δ1 leu2Δ0/leu2Δ0 lys2Δ0/LYS2 met15Δ0/MET15 ura3Δ0/ura3Δ0* | M. Aigle, derived from ref. 1. |
| GY815 | 4N | S288c | ***MATa/MATa/MATalpha/MATalpha****his3Δ1/his3Δ1/his3Δ1/his3Δ1 leu2Δ0/leu2Δ0/ leu2Δ0/leu2Δ0 lys2Δ0/LYS2/lys2Δ0/LYS2 met15Δ0/MET15/met15Δ0/MET15 ura3Δ0/ura3Δ0/ura3Δ0/ura3Δ0* | M. Aigle, derived from ref. 1. |
| GY816 | 3N | S288c | ***MATalpha/MATalpha/MATa*** *his3Δ1/his3Δ1/his3Δ1 leu2Δ0/leu2Δ0/leu2Δ0 lys2Δ0/ LYS2/LYS2 met15Δ0/MET15/met15Δ0 ura3Δ0/ura3Δ0/ura3Δ0* | M. Aigle, derived from ref. 1. |
| GY880 | 1N | A364a | ***MATalpha****cdc28-4* | N. Grandin, derived from ref. 2. |

1 Storchova Z, et al. (2006) Genome-wide genetic analysis of polyploidy in yeast. *Nature* 443:541–547.
2 Reed SI, Hadwiger JA, Lorincz AT (1985) Protein kinase activity associated with the product of the yeast cell division cycle gene CDC28. *Proc Natl Acad Sci USA* 82:4055–4059.